ACS Catalysis

Letter

pubs.acs.org/acscatalysis

Direct Access to Oxidation-Resistant Nickel Catalysts through an Organometallic Precursor

Natália J. S. Costa,[†] Renato F. Jardim,[‡] Sueli H. Masunaga,[‡] Daniela Zanchet,[§] Richard Landers,[⊥] and Liane M. Rossi*[,†]

[†]Instituto de Química, Universidade de São Paulo, 05508-000 São Paulo, SP, Brazil

[‡]Instituto de Física, Universidade de São Paulo, 05315-970 São Paulo, SP, Brazil

[§]Instituto de Química, [⊥]Instituto de Física, UNICAMP, 13083-970 Campinas, SP, Brazil

Supporting Information

ABSTRACT: The synthesis of nickel catalysts for industrial applications is relatively simple; however, nickel oxidation is usually difficult to avoid, which makes it challenging to optimize catalytic activities, metal loadings, and high-temperature activation steps. A robust, oxidation-resistant and very active nickel catalyst was prepared by controlled decomposition of the organometallic precursor [bis(1,5-cyclooctadiene)nickel(0)], Ni(COD)$_2$, over silica-coated magnetite (Fe_3O_4@SiO_2). The sample is mostly Ni(0), and surface oxidized species formed after exposure to air are easily reduced in situ during hydrogenation of cyclohexene under mild conditions recovering the initial activity. This unique behavior may benefit several other reactions that are likely to proceed via Ni heterogeneous catalysis.

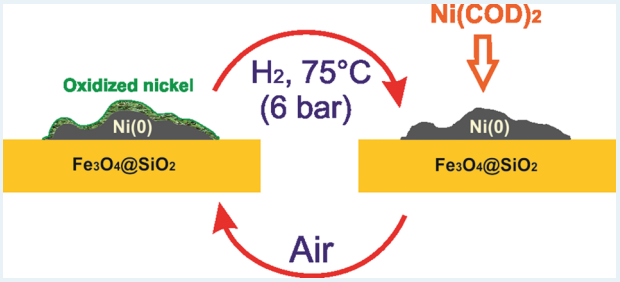

KEYWORDS: *nickel nanoparticles, organometallic, Ni(COD)$_2$, hydrogenation, magnetic separation*

The synthesis of nickel(0) nanoparticles (NiNPs) with clean surfaces is hindered by the propensity of nickel to oxidize. Strong reducing and protective agents modify the metal surfaces and may affect the catalytic properties of the NPs. If metal oxidation occurs, harsh reaction conditions will be required for nickel oxide reduction back to the most active Ni(0) form. An organometallic approach has offered an excellent route for controlling the surface chemistry of NPs.[1] The olefinic ligands of organometallic precursors are reduced, and the naked atoms condense, producing metal NPs with clean and unoxidized metal surfaces. To avoid the formation of bulk metal, different stabilizing methods can be applied. The organometallic compound [bis(1,5-cyclooctadiene) nickel(0)], Ni(COD)$_2$, decomposes to prepare NiNPs for different applications.[2−11] Chaudret's group synthesized NiNPs using a solution containing Ni(COD)$_2$, a stabilizing agent, and moderate H_2 pressure (3 bar) at room temperature.[6−8,10] Migowski et al. prepared Ni(0) catalysts through decomposition of Ni(COD)$_2$ in imidazolium ionic liquids. However, the NiNPs exhibit moderate activity in the hydrogenation of cyclohexene in biphasic catalysis (turnover frequency of 91 h^{-1}).[11] NiNPs were also prepared by autodecomposition of Ni(COD)$_2$ in imidazolium ionic liquids in the absence of classical reducing agents.[12] We report herein the synthesis of supported NiNPs performed under controlled hydrogen reduction of the cyclooctadiene ligands of Ni(COD)$_2$ and the subsequent deposition of nickel nanoaggregates over a magnetic catalyst support (Fe_3O_4@SiO_2).[13] The NiNPs are resistant to oxidation (surface oxidation only), magnetically recoverable, more active than the commercial Raney Ni catalyst in hydrogenations, and should be of interest for several other useful reactions that are likely to proceed via Ni heterogeneous catalysis; for example, C−C and C-heteroatom couplings.[14]

NiNP catalysts were prepared by adding a cyclohexene solution of Ni(COD)$_2$ (nominal 2 wt % Ni) to the catalyst supports (Fe_3O_4, SiO_2, and Fe_3O_4@SiO_2 prepared according to reference 13) in a Fischer−Porter glass reactor. All transfers were made under inert conditions in a glovebox. The reactor was connected to a pressurized hydrogen gas tank, the hydrogen gas was admitted, and the catalyst was formed under constant pressure and temperature. After an initial activation time without changes in the hydrogen pressure, the hydrogenation of cyclohexene started as observed through the consumption of hydrogen, which is an indication of the formation of NiNPs as an active catalytic phase (Figure 1). The solution changed from yellow to colorless, further indicating the deposition of nickel on the solid support. The catalyst support containing magnetite nanoparticles spherically coated by silica, Fe_3O_4@SiO_2, formed the most active Ni(0) catalyst and was chosen for further studies.

Received: November 23, 2011
Revised: April 4, 2012
Published: April 18, 2012

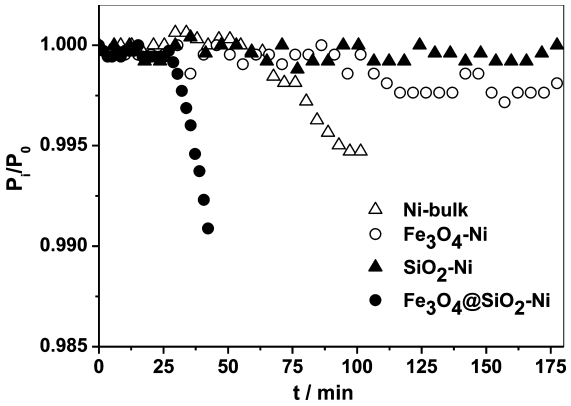

Figure 1. Hydrogen gas consumption profile during the deposition of $Ni(COD)_2$ in different supports in the presence of cyclohexene. p_i = initial H_2 pressure in the hydrogen gas supplier tank and p_0 = H_2 gas pressure in a given time. Conditions: 3 bar H_2 (constant), 27 °C, 100 mg of support, 12.5 mg $Ni(COD)_2$, and 2.5 mL of cyclohexene.

The preparation of NiNPs on Fe_3O_4@SiO_2 using different hydrogen pressures (p) and temperatures (T) is shown in Table 1. The catalytic performance of the catalysts prepared under different conditions was tested in the hydrogenation of the model substrate cyclohexene using similar reaction conditions (300 $mol_{substrate}/mol_{catalyst}$ at 75 °C and under 6 bar of H_2). The catalytic reactions were monitored by the fall in the pressure of the hydrogen gas supply over time until completion (>99%, confirmed by GC after the hydrogen consumption ceased). The catalyst synthesized at higher T and p (Table 1, entry 1) was found to be less active than those prepared under either lower T (Table 1, entry 2), p (Table 1, entry 3), or both (Table 1, entry 4). In addition, the supported catalyst prepared under mild conditions (Table 1, entry 4) is more active than the Ni bulk prepared by decomposition of $Ni(COD)_2$ without support (Table 1, entry 6). The catalyst prepared under mild conditions (3 bar H_2 and 27 °C) was further investigated in the hydrogenation of cyclohexene under various reaction conditions (Table 1, entries 7–12). The hydrogenation reactions using 0.33 mol % Ni reached >99% conversion in less than 1 h under hydrogen pressure as low as 1 bar and 27 °C. As expected, the reaction rates increase with p or T.

Table 1. Synthesis and Catalytic Activity of NiNPs Prepared by Deposition of $Ni(COD)_2$ on Fe_3O_4@SiO_2 under Different p and T Conditions

	catalyst synthesis[a]		catalytic reactions[b]			
entry	p (bar)	T (°C)	p (bar)	T (°C)	time[c] (min)	TOF[d] (h^{-1})
1	6	75	6	75	43	264
2	6	27	6	75	12	1500
3	3	75	6	75	11	1000
4	3	27	6	75	11	1111
5[e]	6	75	6	75	41	513
6[e]	3	27	6	75	19	706
7	3	27	1	75	58	254
8	3	27	3	75	21	653
9	3	27	5	75	12	1181
10	3	27	6	27	33	398
11	3	27	6	45	27	588
12	3	27	6	90	11	1579

[a]12.5 mg of $Ni(COD)_2$, Fe_3O_4@SiO_2 (100 mg), 2.5 mL of cyclohexene. [b]1.1 g of cyclohexene, 100 mg catalyst (300 mol of substrate per mol of Ni). [c]Reaction time to reach >99% conversion. [d]TOF = mol of substrate converted per mol of catalyst (total amount) per hour at 20% conversion. [e]Ni bulk prepared by decomposition of $Ni(COD)_2$ without support.

Alonso and co-workers have used Ni NPs for hydrogenation of organic compounds by hydrogen transfer reactions in replacement of noble metals.[15−18] However, the performance of nickel in liquid phase hydrogenation reactions using H_2 as a reducing agent is usually poor when compared with noble metals. NiNPs prepared by reducing $NiCl_2$ with hydrazine in methanol exhibited catalytic activity in the hydrogenation of alkynes, reaching a conversion of 98% in 24 h at 7 bar of H_2 and room temperature.[19] Clay-entrapped NiNPs, prepared by reducing Ni^{2+}-exchanged K10-montmorillonite, converted 52% of cyclohexene into cyclohexane after 8 h using hydrazine as a reducing agent.[20] A catalyst prepared by impregnating presynthesized NiNPs in silica and carbon does not exhibit catalytic activity in the hydrogenation of cyclohexene under 10 bar of H_2 and 100 °C.[21] NiNPs prepared through decomposition of $Ni(COD)_2$ in imidazolium ionic liquids last 14 h to hydrogenate cyclohexene (13 mmol, substrate/Ni = 250) in biphasic conditions under 100 °C and 4 bar H_2.[11]

Our supported NiNPs obtained through the organometallic precursor (Fe_3O_4@SiO_2Ni) exhibit higher reaction rates (turnover frequencies as high as 1500 h^{-1}) than those reported for Ni catalysts, which are much closer to the rates of supported noble metal nanoparticles reported for this model reaction (Fe_3O_4@SiO_2Ru,[22] Fe_3O_4@SiO_2Pt[23]). We also tested the catalytic activity of the widely used Raney nickel (a moisture sensitive and pyrophoric catalyst) in the hydrogenation of cyclohexene under similar conditions (0.33 mol % of Ni, 75 °C, and 6 bar H_2), but reaction rates were very low (29% conversion after 48 h of reaction). Conversion as high as 90% in 2 h has been reported using 5 mol % of Ni,[9] which corresponds to more than 10 times the amount of catalyst used in our studies.

The catalyst Fe_3O_4@SiO_2Ni was recycled by magnetic separation and tested in successive hydrogenation reactions without being removed from the reactor (Figure 2). This procedure minimizes exposure to air and prevents catalyst

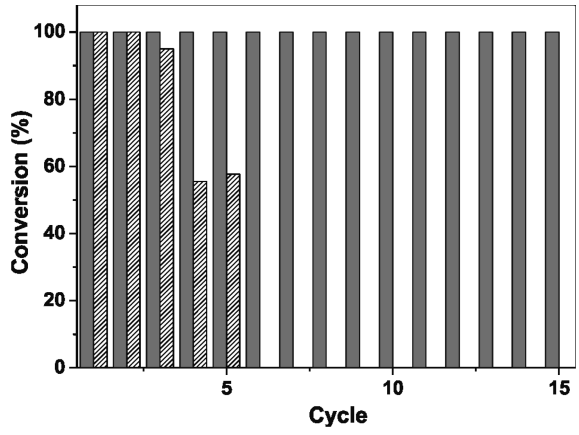

Figure 2. Recycling studies of Ni bulk (dashed) and Fe_3O_4@SiO_2Ni (solid) catalysts in successive hydrogenations of cyclohexene. Reaction conditions: 1.1 g of cyclohexene, 100 mg of catalyst (cyclohexene/Ni = 300), 6 bar of H_2, at 75 °C, and 25 min.

dx.doi.org/10.1021/cs200609e | ACS Catal. 2012, 2, 925−929

oxidation. The supported catalyst could be recycled in successive hydrogenation reactions reaching >99% conversion for up to 15 cycles or 4500 $mol_{substrate}/mol_{catalyst}$ without deactivation. The results for Ni bulk catalyst are included for comparison. The Ni content found in the organic phase after the recycles was ~4 ppm for Ni bulk (nonsupported) and <0.01 ppm for Fe_3O_4@SiO_2Ni. The excellent catalytic performance and the lack of Ni leaching of Fe_3O_4@SiO_2Ni confirmed the importance of the support for the stabilization of the NiNPs.

Because the performance of nickel catalysts may be affected to some extent by their propensity to oxidation, we tested the catalytic activity of the Fe_3O_4@SiO_2Ni catalyst after its exposure to air. In a first set of experiments, the catalyst was synthesized in the normal manner and used to hydrogenate cyclohexene (Figure 3, curve a). The reactor was opened, and

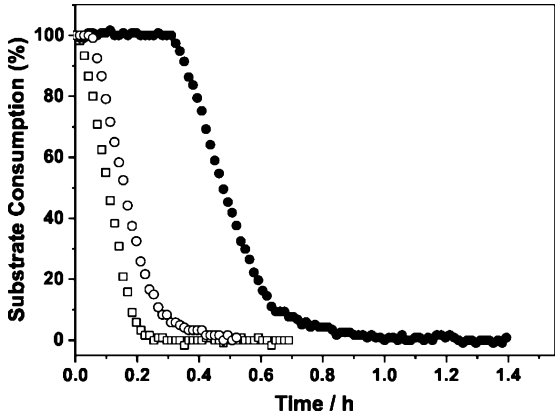

Figure 3. Hydrogenation curves: (a, □) fresh catalyst, (b, ●) catalyst after exposure to air for 72 h (first reaction), (c, ○) catalyst after exposure to air for 72 h (second reaction). Reaction conditions: 100 mg of catalyst and 1.1 g of cyclohexene, 6 bar of H_2, and 75 °C.

the catalyst was exposed to air. After the desired time (72 h), the reactor was loaded with cyclohexene and hydrogen gas for the next reaction. After an activation time of 0.4 h, the catalyst recovered its activity (Figure 3, curve b). In the third run (Figure 3, curve c), the behavior of the catalyst reactivated in situ was similar to the fresh catalyst prepared under controlled conditions. The Fe_3O_4@SiO_2Ni catalyst exposed to air for up to a couple of months could also be reactivated by submitting the powder to hydrogen gas (1 bar) and 75 °C for 1 h previous to the liquid phase reactions. The results suggest that if surface oxidized species are formed upon exposure to air, they can be easily reduced back to an active Ni(0) catalyst under the reaction conditions, recovering the initial catalyst activity.

In general, after oxidation, Ni catalysts need to be activated before use. The methodology for such a procedure includes heat treatment in the presence of hydrogen gas at temperatures ranging from 250 °C (in acid slurry) to 500 °C,[24−31] which are harsher than the reaction conditions used in this study. The behavior of the catalyst Fe_3O_4@SiO_2Ni becomes more important after analysis of the other two catalysts: (i) supported NiO catalyst synthesized by wet impregnation of $Ni(NO_3)_2$ in the Fe_3O_4@SiO_2 support, followed by calcination in air for 2 h at 500 °C (Fe_3O_4@SiO_2−NiO); and (ii) commercially available NiO. The two catalysts were tested under similar conditions (0.33 mol % catalyst, 6 bar of H_2, and at 75 °C), and no reaction was observed in the following 24 h, further indicating that they were not reduced under the studied conditions.

The catalyst was characterized by different techniques to identify the nickel phase present after exposure to air. The transmission electron microscopy (TEM) and high resolution TEM (HRTEM) images of Fe_3O_4@SiO_2Ni in Figure 4a and b

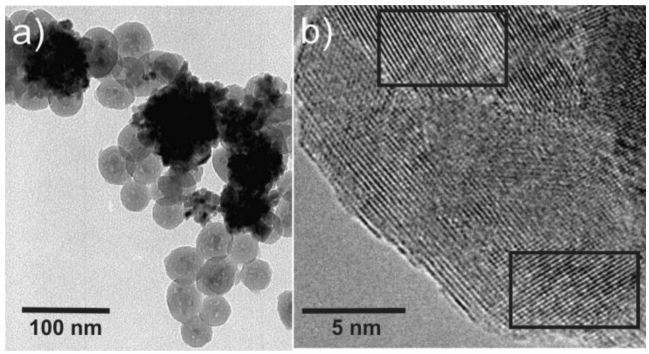

Figure 4. (a) TEM and (b) HRTEM images of Fe_3O_4@SiO_2Ni. The selected areas shown in part b were used for interplanar distance determination.

reveal the morphology of the core−shell magnetic support and the NiNPs. The iron oxide NPs of ~10 nm are spherically coated by silica, resulting in ~45 nm silica spheres. The Ni metal was deposited on the support surface as aggregates (Figure 4a). The HRTEM image in Figure 4b reveals lattice spacing of 2.03 Å for the two highlighted areas, which corresponds to the interplanar distance (1 1 1) of Ni(0) in a cubic system (JCPDS #011260), with an experimental error of <1%. The main *hkl* planes of Ni(0) in a cubic system were also found in the diffraction ring patterns obtained in selected areas electron diffraction (SAED) (see Supporting Information Figure S1).

The magnetic properties of the catalyst that render magnetic separation at the end of the reactions and during workup procedures arise from two contributions: the iron oxide NPs of the support and the NiNPs. Therefore, it was necessary to take into account the magnetic contribution of both NPs for the analysis of the magnetic properties of the supported nickel catalyst. At this point, it is important to mention that the presence of magnetite in the silica support (~9 wt %) is necessary for magnetic separation because the Ni loading (~2 wt %) is not sufficient to separate magnetically all the silica used as a support. To investigate the magnetic properties of this material, magnetization curves $M \times H$ of the magnetic support (Fe_3O_4@SiO_2) and the catalyst (Fe_3O_4@SiO_2Ni) were recorded at room temperature. According to the magnetization curve of the Ni catalyst contribution obtained after subtracting the magnetite contribution (Figure 5), a saturation magnetization of 52 emu g^{-1} was estimated, a value that agrees with the presence of Ni(0),[32] within 10% error in the magnetic material mass determination. The magnetic contribution in the case of sample oxidation would be much lower than that obtained here.[33] Moreover, the saturation magnetization of the subtracted $M \times H$ curve further indicated that the sample is Ni(0) NPs, since no saturation magnetization is expected for nickel oxides in similar applied magnetic fields and at 27 °C.[34−37] The results obtained from HRTEM, SAED, and magnetic measurements indicate that the sample consists mostly of Ni(0); however, considering the limitations of each

dx.doi.org/10.1021/cs200609e | ACS Catal. 2012, 2, 925−929

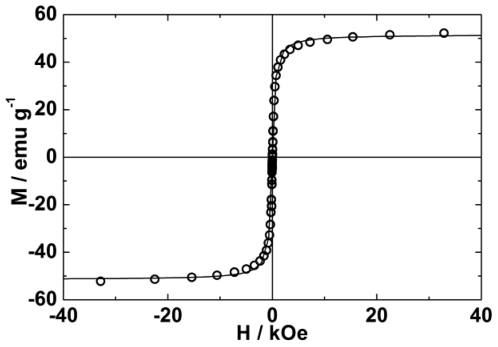

Figure 5. Magnetization curve $M \times H$ of Ni aggregates in Fe_3O_4@SiO_2Ni at 27 °C.

technique, we cannot exclude the presence of a thin layer of oxidized species on our samples.

To obtain further information on the electronic character of the nickel present in Fe_3O_4@SiO_2Ni after exposure to air, the sample was analyzed by X-ray absorption near edge structure (XANES) and by X-ray photoelectron spectroscopy (XPS), one of the most widely used surface chemical analysis techniques. Figure 6a shows the XANES compared to the Ni foil and NiO standards. The results indicate the presence of Ni(0), but do not exclude surface oxidation by a small increase in the unoccupied density of state compared with the Ni metal. Figure 6b shows the XPS analysis of Fe_3O_4@SiO_2Ni. The spectrum of the Ni 2p3/2 region confirmed the presence of Ni(0) with a peak binding energy at 853.2 eV, corresponding to zerovalent metallic nickel, and confirmed the presence of oxidized nickel with a peak binding energy at 855.9 eV and its corresponding shakeup resonance at 861.1 eV.[38]

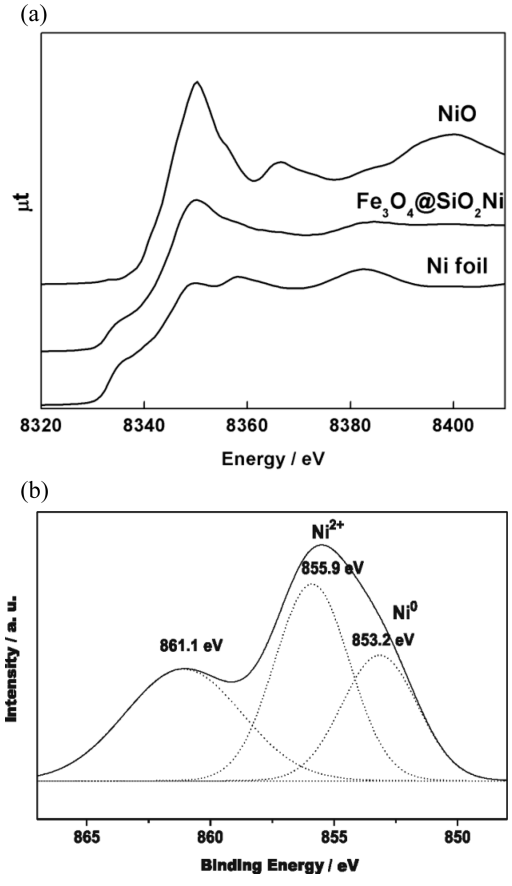

Figure 6. (a) XANES of Fe_3O_4@SiO_2Ni, NiO, and Ni foil. (b) XPS spectrum of Ni2$p_{3/2}$ region of Fe_3O_4@SiO_2Ni.

In summary, the organometallic approach represents a robust strategy for preparing surfactant-free NiNPs that are either resistant to oxidation, allowing the preparation of highly active nickel catalysts, or are easily reactivated in situ, recovering its catalytic activity, after exposure to air. Partial surface oxidation could be detected after storage in air, but the catalytic results indicate that these oxidized nickel species can be reduced back to the Ni(0) active catalyst under hydrogenation reaction conditions (6 bar of H_2 and 75 °C), in contrast with NiO bulk. The turnover frequencies (as high as 1500 h^{-1}) and the recycling properties (4500 mol/mol Ni, not optimized) can be compared with the catalytic rates of noble metals reported for this model reaction. Moreover, several other useful reactions that are likely to proceed via Ni heterogeneous catalysis are currently under investigation.

■ ASSOCIATED CONTENT

Supporting Information

Experimental details and catalyst characterization. This material is available free of charge via the Internet at http://pubs.acs.org.

■ AUTHOR INFORMATION

Corresponding Author

*Phone: +55 11 30919143. Fax: +55 11 38155579. E-mail: lrossi@iq.usp.br. Address: Instituto de Química, Universidade de São Paulo, Av. Prof. Lineu Prestes 748, São Paulo 05508-000, SP, Brazil.

Notes

The authors declare no competing financial interest.

■ ACKNOWLEDGMENTS

We thank FAPESP, CAPES, CNPq, and INCT-Catalise for financial support and the Brazilian Synchrotron Light Laboratory, Campinas–SP for use of the TEM and XAFS facilities.

■ REFERENCES

(1) Chaudret, B. *C. R. Phys.* **2005**, *6*, 117.
(2) Dire, S.; Ceccato, R.; Facchin, G.; Carturan, G. *J. Mater. Chem.* **2001**, *11*, 678.
(3) Zhu, K.; D'Souza, L.; Richards, R. M. *Appl. Organomet. Chem.* **2005**, *19*, 1065.
(4) Rodriguez-Llamazares, S.; Merchan, J.; Olmedo, I.; Marambio, H. P.; Munoz, J. P.; Jara, P.; Sturm, J. C.; Chornik, B.; Pena, O.; Yutronic, N.; Kogan, M. J. *J. Nanosci. Nanotechnol.* **2008**, *8*, 3820.
(5) Ramirez-Meneses, E.; Betancourt, I.; Morales, F.; Montiel-Palma, V.; Villanueva-Alvarado, C. C.; Hernandez-Rojas, M. E. *J. Nanopart. Res.* **2011**, *13*, 365.
(6) Ould-Ely, T.; Amiens, C.; Chaudret, B.; Snoeck, E.; Verelst, M.; Respaud, M.; Broto, J. M. *Chem. Mater.* **1999**, *11*, 526.
(7) Cordente, N.; Amiens, C.; Chaudret, B.; Respaud, M.; Senocq, F.; Casanove, M. J. *J. Appl. Phys.* **2003**, *94*, 6358.
(8) Cordente, N.; Respaud, M.; Senocq, F.; Casanove, M. J.; Amiens, C.; Chaudret, B. *Nano Lett.* **2001**, *1*, 565.
(9) Domínguez-Crespo, M. A.; Ramirez-Meneses, E.; Montiel-Palma, V.; Huerta, A. M. T.; Rosales, H. D. *Int. J. Hydrogen Energy* **2009**, *34*, 1664.
(10) Ely, T. O.; Amiens, C.; Chaudret, B.; Snoeck, E.; Verelst, M.; Respaud, M.; Broto, J. M. *Chem. Mater.* **1999**, *11*, 526.

(11) Migowski, P.; Machado, G.; Texeira, S. R.; Alves, M. C. M.; Morais, J.; Traverse, A.; Dupont, J. *Phys. Chem. Chem. Phys.* **2007**, *9*, 4814.
(12) Prechtl, M. H. G.; Campbell, P. S.; Scholten, J. D.; Fraser, G. B.; Machado, G.; Santini, C. C.; Dupont, J.; Chauvin, Y. *Nanoscale* **2010**, *2*, 2601.
(13) Jacinto, M. J.; Kiyohara, P. K.; Masunaga, S. H.; Jardim, R. F.; Rossi, L. M. *Appl. Catal., A* **2008**, *338*, 52.
(14) Frieman, B. A.; Taft, B. R.; Lee, C.-T.; Butler, T.; Lipshutz, B. H. *Synthesis* **2005**, *17*, 2989.
(15) Alonso, F.; Riente, P.; Yus, M. *Acc. Chem. Res,* **2011**, *44*, 379.
(16) Alonso, F.; Riente, P.; Sirvent, J. A.; Yus, M. *Appl. Catal., A* **2010**, *378*, 42.
(17) Alonso, F.; Osante, I.; Yus, M. *Tetrahedron* **2007**, *63*, 93.
(18) Alonso, F.; Riente, P.; Yus, M. *Tetrahedron* **2009**, *65*, 10637.
(19) Polshettiwar, V.; Baruwati, B.; Varma, R. S. *Green Chem.* **2009**, *11*, 127.
(20) Dhakshinamoorthy, A.; Pitchumani, K. *Tetrahedron Lett.* **2008**, *49*, 1818.
(21) Rinaldi, R.; Porcari, A. D.; Rocha, T. C. R.; Cassinelli, W. H.; Ribeiro, R. U.; Bueno, J. M. C.; Zanchet, D. *J. Mol. Catal. A: Chem.* **2009**, *301*, 11.
(22) Jacinto, M. J.; Santos, O. H. C. F.; Jardim, R. F.; Landers, R.; Rossi, L. M. *Appl. Catal., A* **2009**, *360*, 177.
(23) Jacinto, M. J.; Landers, R.; Rossi, L. M. *Catal. Commun.* **2009**, *10*, 1971.
(24) Ahn, J. G.; Hai, H. T.; Kim, D. J.; Park, J. S.; Kim, S. B. *Hydrometallurgy* **2010**, *102*, 101.
(25) Espinos, J. P.; Gonzalez-Elipe, A. R.; Caballero, A.; Garcia, J.; Munuera, G. *J. Catal.* **1992**, *136*, 415.
(26) Floquet, N.; Dufour, L. C. *Surf. Sci.* **1983**, *126*, 543.
(27) Li, H.; Yu, D. H.; Hu, Y.; Sun, P.; Xia, J. J.; Huang, H. *Carbon* **2010**, *48*, 4547.
(28) L'Vov, B. V.; Russ., J. *Appl. Chem.* **2010**, *83*, 778.
(29) Mile, B.; Stirling, D.; Zammitt, M. A.; Lovell, A.; Webb, M. *J. Catal.* **1988**, *114*, 217.
(30) Richardson, J. T.; Turk, B.; Lei, M.; Forster, K.; Twigg, M. V. *Appl. Catal., A* **1992**, *83*, 87.
(31) Roman, A.; Delmon, B. *J. Catal.* **1973**, *30*, 333.
(32) Cullity, B. D.; GrahamC. D.*Introduction to Magnetic Materials*; 2nd ed.; John Wiley & Son, 2009.
(33) Kodama, R. H.; Makhlouf, S. A.; Berkovitz, A. E. *Phys. Rev. Lett.* **1997**, *79*, 1393.
(34) Fonseca, F. C.; Jardim, R. F.; Escote, M. T.; Gouveia, P. S.; Leite, E. R.; Longo, E. *J. Nanopart. Res.* **2011**, *13*, 703.
(35) Ichiyanagi, Y.; Wakabayashi, N.; Yamazaki, J.; Yamada, S.; Kimishima, Y.; Komatsu, E.; Tajima, H. *Phys. B (Amsterdam, Neth.)* **2003**, *329*, 862.
(36) Karthik, K.; Selvan, G. K.; Kanaga-raj, M.; Arumugam, S.; Jaya, N. V. *J. Alloys Compd.* **2011**, *509*, 181.
(37) Sun, X. C.; Dong, X. L. *Mater. Res. Bull.* **2002**, *37*, 991.
(38) Koltypin, Y.; Fernandez, A.; Rojas, T. C.; Campora, J.; Palma, P.; Prozorov, R.; Gedanken, A. *Chem. Mater.* **1999**, *11*, 1331.